Article ID: 1006-8775(2010) 04-0313-12

MODIS BRIGHTNESS TEMPERATURE DATA ASSIMILATION UNDER CLOUDY CONDITIONS: METHODS AND IDEAL TESTS

DING Wei-yu (丁伟钰), WAN Qi-lin (万齐林), ZHANG Chen-zhong (张诚忠), CHEN Zi-tong (陈子通), HUANG Yan-yan (黄燕燕)

(Guangzhou Institute of Tropical and Marine Meteorology, China Meteorological Administration, Guangzhou 510080 China)

Abstract: Clouds have important effects on the infrared radiances transmission in that the inclusion of cloud effects in data assimilation can not only improve the quality of the assimilated atmospheric parameters greatly, but also minimize the initial error of cloud parameters by adjusting part of the infrared radiances data. On the basis of the Grapes-3D-var (Global and Regional Assimilation and Prediction Enhanced System), cloud liquid water, cloud ice water and cloud cover are added as the governing variables in the assimilation. Under the conditions of clear sky, partly cloudy cover and totally cloudy cover, the brightness temperature of 16 MODIS channels are assimilated respectively in ideal tests. Results show that when the simulated background brightness temperatures are lower than the observation, the analyzed field will increase the simulated brightness temperature by increasing its temperature and reducing its moisture, cloud liquid water, cloud ice water, and cloud cover. The simulated brightness temperature can be reduced if adjustment is made in the contrary direction. The adjustment of the temperature and specific humidity under the clear sky conditions conforms well to the design of MODIS channels, but it is weakened for levels under cloud layers. The ideal tests demonstrate that by simultaneously adding both cloud parameters and atmospheric parameters as governing variables during the assimilation of infrared radiances, both the cloud parameters and atmospheric parameters can be adjusted using the observed infrared radiances and conventional meteorological elements to make full use of the infrared observations.

Key words: cloud parameters; MODIS brightness temperature data; assimilation

CLC number: P412.27 **Document code:** A **doi:** 10.3969/j.issn.1006-8775.2010.04.002

1 INTRODUCTION

The use of variational methods to assimilate observational information in the field of atmospheric sciences has a wide range of applications. These methods play important roles in the analysis of meteorological elements[1, 2], atmospheric tracer gas[3], and the carbon cycle[4], among others. Based on certain objective criteria, variational assimilation methods can integrate background and observational information to obtain information that cannot be directly inferred from observational data. For example, Li et al.[5] used Geostationary Operational Environmental Satellites (GOES) radiation data to correct the first-guessed cloud height and cloud cover through a one-dimensional variational assimilation method. The method is more accurate than the CO_2 slice method.

Using variational assimilation methods to assimilate satellite radiation data directly is the trend in satellite data assimilation. As opposed to the method of assimilating retrieved satellite data, radiance data assimilation can reduce intermediate processes, including additional errors. As such, this method has been used in numerous studies. Andersson et al.[6] used a three/four-dimensional variational data assimilation scheme to assimilate radiation data and improve wind forecasts. Okamoto and Derber[7] assimilated SSM/I radiation data in the NCEP global model. Numerous studies have also been conducted in China. For example, Wang[8] discussed the reasons for using direct radiance data assimilation, rather than retrieved satellite data assimilation, in numerical weather prediction, the role of direct variational assimilations in radiance data applications, and the adjoint method in

Received date: 2010-03-02; **revised date:** 2010-08-17

Foundation item: Speical Scientific Research Project for Public Welfare (Meteorological) Industry (GYHY200906002); Project of National Natural Science Foundation (41075083)

Biography: DING Wei-yu, M.S., primarily undertaking research on forecasting techniques of tropical meteorology.

E-mail for corresponding author: wyding@grmc.gov.cn

variational data assimilation. Pan et al.[9] used an incremental three-dimensional variational (3D-Var) assimilation method to assimilate Advanced Microwave Sounding Unit-A (AMSU-A) brightness temperature data and radiosonde data. They also compared assimilation and forecast results from the MM5 mesoscale model. Zhang et al.[10] used the Global and Regional Assimilation Prediction System (GRAPES) 3D-var system to assimilate ATOVS radiation data directly and to improve track forecasts on Typhoon Rammasun.

However, these numerous studies have failed to consider the impact of clouds on the radiation process. Instead, rejecting observations under cloudy conditions have led to the use of satellite infrared data, which are very limited in the tropics, during typhoons and torrential rains. Some experiments using infrared data assimilation under cloudy conditions have been conducted. Thomas et al.[11] developed an observational operator to be used in radiance assimilation under all weather conditions. They used a radiative transfer model, a gas extinction model, and a cloud model to generate required information on the physical quantities of clouds. GOES-9 brightness temperatures were assimilated through the four-dimensional variational assimilation system using this observational operator, together with an improved surface-layer cloud system simulation. Ding and Wan[12] used fast radiative transfer model for TOVS (RTTOV) to simulate high-resolution infrared radiation sounder (HIRS) observations on the spiral structure of typhoons. Results showed that cloud parameters have a very significant impact on the simulation. These studies indicate that infrared radiation data have potential applications under cloudy and extreme weather conditions.

Errors in the numerical model simulation of clouds exist. To a certain extent, the addition of cloud parameters, as constants, to the assimilation system can improve the assimilation effect. Errors of cloud parameters affect the results of the atmospheric parameters assimilation. Therefore, it is necessary to include them as variables in assimilation systems. Infrared data can retrieve the macro-characteristics of clouds[13]. Initial errors of cloud parameters can be reduced with the addition of cloud parameters as variables to the assimilation system, and with the use of infrared data to adjust them, thus improving the assimilation of atmospheric parameters. Moderate-resolution imaging spectroradiometer (MODIS) is one of the most distinctive instruments in the Earth Observing System (EOS) Program (1991–2013) of the United States. Its 16 infrared channels are widely used in the retrieval of atmospheric temperature, humidity profiles, and cloud parameters[14]. MODIS-retrieved data play an important role in data assimilation. For instance, the dataset of Terra–MODIS winds prepared by the Cooperative Institute for Meteorological Satellite Studies (CIMSS) at the University of Wisconsin-Madison markedly improved the forecasting techniques of the European Centre for Medium-Range Weather Forecasts (ECMWF)[15]. No study on the assimilation of MODIS radiance data under cloudy conditions has yet been published. As MODIS has multi-channels and a wide spectrum, research on MODIS radiance data assimilation can provide a reference for other satellite data assimilation.

In this paper, based on GRAPES 3D-Var assimilation system and the characteristics of RTTOV, cloud water content, cloud ice water content, and cloud cover are included as the control variables of the assimilation system. Ideal tests of assimilation are conducted under clear sky, total cloud cover, and partial cloud cover conditions. Moreover, to verify the assimilation scheme, 16 MODIS channels are assimilated in these tests.

2 ASSIMILATION SCHEME DESIGN

A variational data assimilation scheme is usually defined as a cost function (J)

$$J(x)=\frac{1}{2}\left[(x-x_b)^T\mathbf{B}^{-1}(x-x_b)+(H(x)-y_o)^T\mathbf{O}^{-1}(H(x)-y_o)\right] \quad (1)$$

where x is the analyzed variable, x_b is the background field, y_o is the observed value, H is the observation operator, B is the background error covariance matrix, and O is the observation error covariance matrix. The cost function (J) contains both background and observational information. The data are assimilated by calculating the minimum value of J to determine the distribution of x. The analyzed field contains background and observational information. There are many types of observational data, and the relationship with background elements may not be the same. Hence, different observation operators can serve as links between observations and the background field. GRAPES 3D-Var uses RTTOV as an observation operator to assimilate satellite radiation data directly. RTTOV can convert conventional meteorological fields to satellite brightness temperature or radiance, establishing contact with satellite observations. This article is based on the GRAPES 3D-Var system, RTTOV, and the characteristics of MODIS data. It uses the following schemes to adjust the GRAPES 3D-Var system.

Developed in the early 1990s by the European Centers for Medium-Range Weather Forecast (ECMWF) for the simulation of TOVS as a rapid

radiative transfer model, RTTOV has been improved to simulate a variety of infrared and microwave channels of weather satellites. It is used to assess the Earth's environment. The spectral range of RTTOV is 3–20 μm in the infrared channels and 10–200 GHz in the microwave channels[21]. The top-of-atmosphere upwelling radiance is written as

$$L(\nu,\theta) = (1-N)L^{Clr}(\nu,\theta) + NL^{Cld}(\nu,\theta) \quad (2)$$

where ν is the frequency of satellite observation, θ is the viewing angle, L^{Clr} and L^{Cld} are the clear sky and fully cloudy top-of-atmosphere upwelling radiances, respectively, and N is the fractional cloud cover. For N, if the cloud cover parameter is set to zero, the radiance will be computed for clear air. When the cloud cover parameter is not zero, radiance will be calculated above the cloud top and under clear conditions based on the ratio of cloud cover. In the preliminary work of our research[12], RTTOV was used to simulate the HIRS brightness temperature of Typhoon Chanchu. Results showed that cloud parameters strongly influence the simulation of infrared brightness temperature. MODIS channels for meteorological observations belong to the infrared channels. The original GRAPES 3D-Var system does not take into account the impact of clouds when assimilating infrared radiance, and rejects the data affected by clouds. Therefore, according to the radiance assimilation scheme of the GRAPES 3D-Var system, the use of infrared data in the tropics or during typhoons, rainstorms, and other extreme weather conditions is limited. In this work, the numerical simulation of cloud parameters is added to the observation operator (RTTOV). This improves the simulation of infrared brightness temperature and enhances data utilization.

The GRAPES 3D-Var system consists of four control variables: the mass field (temperature or geopotential height), water vapor field (specific humidity or relative humidity), and the U and V components of wind. Taking into account the cloud parameters (cloud water content, cloud ice content, and cloud cover) in the process of assimilating satellite infrared radiance, clouds play a very important role. Initial cloud parameters may not be accurate if they are used as constants, and their errors may affect the analyzed temperature, water vapor, and other physical elements. It is necessary to adjust cloud parameters in the process of satellite radiance data assimilation. Research has confirmed the impact of initial cloud parameters on numerical simulation. Cloud parameters are adjusted reasonably by satellite radiance assimilation and by improving the initial field. Atmospheric and cloud parameters can be added as variables to RTTOV, the tangent linear model, and the adjoint model. In this work, cloud water content, cloud ice content, and cloud cover are added to the GRAPES 3D-Var system as control variables, together with the four control variables (i.e., temperature, specific humidity, and the U and V components of wind), giving rise to seven control variables in the new assimilation system.

Observation errors arise from both the MODIS and RTTOV simulations; hence, the maximum simulation error for HIRS by RTTOV is approximately 2.5 K. HIRS and MODIS sensors belong to infrared sensors with similar spectral range, and RTTOV simulates HIRS and MODIS sensors through a similar scheme; hence, this article chooses 2.5 K as the MODIS sensor's observation error. Background errors are defined by the NMC method, and the background error for cloud water content, cloud ice content, and cloud cover are defined by 20% of their values. There are two considerations when setting the background errors of cloud parameters. First, according to the cloud cover simulation error analysis conducted by Jakob[16] for the ECMWF, the average simulation error is approximately 10%–15%. Second, Park and Droegemeier[17] used a 3D cloud model to investigate the sensitivity of variational data assimilation and forecast error for a supercell storm. The cost function was found to be most sensitive to temperature, followed in turn by pressure, water vapor, and cloud water. The first three variables exert strong impact on the cost function. The impact of cloud parameter errors on the cost function is smaller than that of other atmospheric parameters; hence, background errors of cloud parameters in this paper are defined according to Jakob. The exact background field errors of cloud parameters are needed for further analysis.

3 DATA DESCRIPTION AND FORWARD MODEL SIMULATION

MODIS measures biological and physical processes on a global basis. The instrument provides long-term observations from which we enhance our understanding of global dynamics and processes occurring at the Earth's surface and at the lower atmosphere. MODIS sensors have many meteorological channels, similar to HIRS, AVHRR, etc., which are widely used in the retrieval of temperature and humidity profiles. Compared with other satellite sensors, MODIS sensors have features such as (1) wide spectral ranges (36 channels), (2) three kinds of spatial resolution (250, 500, and 1 km), (3) 24-h continuous observation, and (4) a wide observing angle, viewing the entire Earth's surface every two days. MODIS sensors have 16 meteorological channels. These channels are used for

the observation of atmospheric temperature, humidity, water content of cirrus vapor, cloud top height, and ozone (see Table 1). RTTOV can simulate the 16 meteorological channels.

In this paper, NCEP 1°×1° reanalysis data are used as the initial field and boundary fields. The Weather Research and Forecasting (WRF) model is used as the forecasting model, with 15 km resolution. The experiment starts at 0000 UTC (Coordinated Universal Time) on 26 May 2007. The 6-h forecast fields (i.e., 0600 UTC on 26 May) are used as the background fields for assimilation. Background information includes temperature, specific humidity, U and V wind field, cloud water content, cloud ice content and cloud cover, surface type, surface temperature, surface pressure, 2 m temperature, 2 m specific humidity, 2 m wind, cloud top pressure, and total cloud cover. The WRF model is designed with a horizontal resolution of 15 km, containing 31 vertical levels. The model uses a single-moment 5-class scheme for cloud micro-physical parameters. This scheme takes into account water vapor, cloud water, rainwater, cloud ice, and snow. Water and ice may coexist. This scheme can provide 3D forecast fields for cloud water content, cloud ice content, and cloud cover[12]. The determination of cloud base and top, as well as the total cloud cover, is found in Ding and Wan[12].

The observational operator plays a very important role in variational assimilation systems. The key problem of this article is whether RTTOV in the GRAPES 3D-Var system can simulate the MODIS brightness temperature under cloudy conditions. Some successful domestic and international experiences on infrared brightness temperature simulation using RTTOV have taken into account the cloud parameters simulated by cloud models or mesoscale models. Preliminary work precedent to this article has successfully simulated the infrared brightness temperature distribution of Typhoon Chanchu observed by HIRS sensors using RTTOV. This paper follows the technical details of the preliminary work to improve the brightness temperature simulation of MODIS sensors. The WRF model is used to simulate atmospheric and cloud parameters, and RTTOV is used to simulate the MODIS brightness temperature.

At 0540 UTC on 26 May 2007, the AQUR satellite took scans through the Guangdong region. MODIS has 110 335 observation points in the study area (15°–35°N, 105°–125°E). The atmospheric and cloud parameters at 0600 UTC on 26 May are simulated by the WRF model and by NCEP data starting 6 hours earlier. Figure 1 shows the distribution of simulated total cloud cover. A cloud system is evident from southwest to northeast in the south of the country.

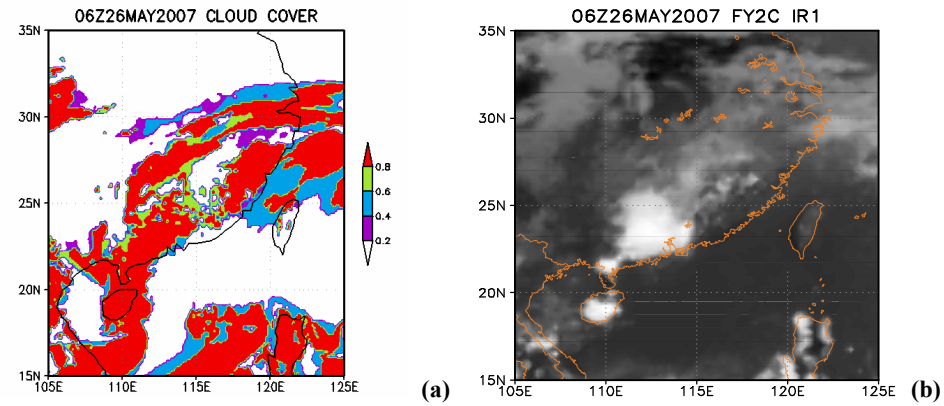

Fig. 1. Total cloud cover simulated by WRF model for 0600 UTC on May 26, 2007 (a); FengYun-2C IR-1 radiance observation (b)

Compared with the FY-2C satellite IR1 channel radiance observation at the time, the WRF model can roughly simulate the distribution of cloud systems; however, there are still some errors in the sea area and Fujian province.

Brightness temperature of each of the 16 MODIS channels listed in Table 1 is simulated by RTTOV in the study area. To compare simulation results, two simulation schemes are used. Atmosphere and cloud parameters are added to RTTOV in the first experiment, while cloud parameters are not included in the second experiment, similar to the observational operator in the GRAPES 3D-Var system. Correlation analysis of the simulated and observed brightness temperature (Table 2) reveals that the correlation coefficients in Exp. 1 are significantly larger than those in Exp. 2 for the 16 channel simulations. This shows that the new simulation scheme is better than the original in the GRAPES 3D-Var system. Channel 29 is designed to observe cloud properties; hence, the simulation of

Channel 29 in Exp. 1 is obviously better than in Exp. 2. Figure 2 shows the observed Channel 29 MODIS brightness temperature and the simulation in Exps 1 and 2. Figure 2 shows that the simulated brightness temperatures in Exp. 2 are higher than observations in cloudy areas; however, it cannot reveal the weather systems in southern China. Due to the distinction between simulated and observed brightness temperature in cloudy regions in Exp. 2, the observational operator cannot be used. This explains why infrared radiance data under cloudy conditions were rejected in the original GRAPES 3D-Var system. Weather systems can easily be found in simulated Channel 29 brightness temperature distributions in Exp. 1. The simulated brightness temperature is close to the observation under cloudy conditions. However, this experiment cannot reflect the extremely low values of brightness temperature in Guangdong province, mainly because of the atmospheric and cloud parameters distribution simulated by the WRF model. The second part of this work adjusts the brightness temperature of the atmospheric and cloud parameters distribution in Guangdong through MODIS assimilation to improve rain and storm forecasts. Other channel simulations are similar to Channel 29. They improve simulations under cloudy conditions in Exp. 1, increasing the strength of correlation between observation and simulation.

Table 1. Characteristics of some MODIS channels and their primary use (bandwidth unit: μm)

Channel	20	21	22	23
bandwidth	3.660~3.840	3.929~3.989	3.929~3.989	4.020~4.080
Primary Use	Surface/Cloud Temperature			
Channel	24	25	27	28
bandwidth	4.433~4.498	4.482~4.549	6.535~6.895	7.175~7.475
Primary Use	Atmospheric Temperature		Cirrus Clouds Water Vapor	
Channel	29	30	31	32
bandwidth	8.400~8.700	9.580~9.880	10.780~11.280	11.770~12.270
Primary Use	Cloud Properties	Ozone	Surface/Cloud Temperature	
Channel	33	34	35	36
bandwidth	13.185~13.485	13.485~13.785	13.785~14.085	14.085~14.385
Primary Use	Cloud Top Altitude			

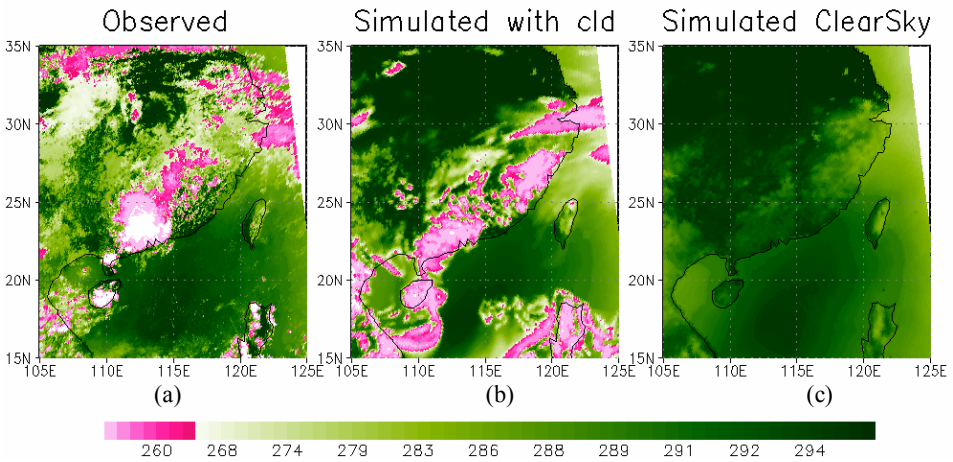

Fig. 2. Brightness temperature observed by a MODIS sensor at channel 29 at 0540 UTC on 26 May 2007 (a); simulated by Test 1 (b); and Test 2 (c). (unit: K)

Table 2. Correlation coefficients between simulation and observation in Exps. 1 and 2 (sample size: 110 335)

Channel	20	21	22	23	24	25	27	28	29	30	31	32	33	34	35	36
Exp. 1	0.45	0.14	0.43	0.42	0.57	0.44	0.45	0.39	0.40	0.40	0.38	0.38	0.45	0.49	0.52	0.64
Exp. 2	0.27	0.01	0.12	0.09	0.43	0.14	0.37	0.25	0.09	0.13	0.12	0.14	0.22	0.27	0.31	0.50

4 DATA ANALYSIS AND SINGLE POINT IDEAL TESTS

Three points have been selected from the WRF model output for the ideal tests: Point A (18°N, 113°E) in clear sky, Point B (23°N, 113°E) in total cloud coverage, and Point C (28°N, 113°E) in partial cloud coverage. The profiles of temperature, humidity, cloud

water content, cloud ice water content, and cloud cover of the three points are shown in Fig. 3. At these points, the temperature profiles are similar. However, humidity profiles vary. For example, the specific humidity between 850–300 hPa at Points B and C is greater than that of Point A because of cloud cover. Point B is completely covered by clouds (with cloud ice) between 500–100 hPa. Clouds at Point C are located in 300–100 hPa and 925–700 hPa, and cloud cover does not exceed 1. There is cloud ice water at higher levels and cloud water at lower levels at Point C; however, cloud ice water content is an order of magnitude lower than at Point B. Single-point assimilation tests are conducted at the three points to reveal the impact of MODIS radiance data on the atmosphere and clouds under different cloud coverage conditions.

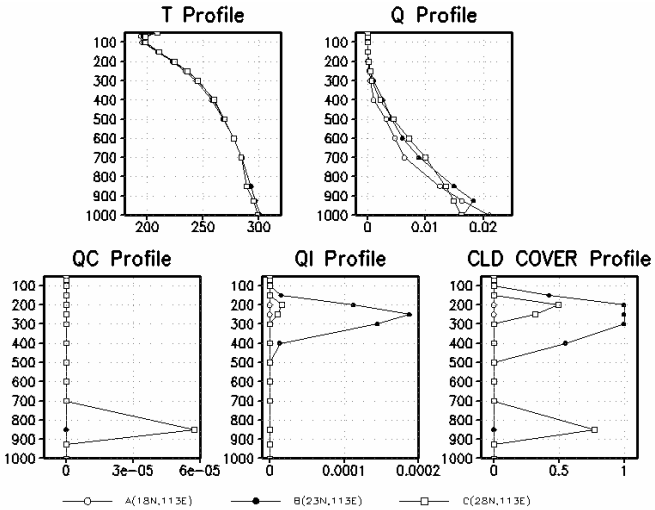

Fig. 3. Profiles of temperature, specific humidity, cloud water content, cloud ice content, and cloud cover in the backgrounds of the three single-point tests

The definition of the initial difference between simulated brightness temperature and observation is as follows:

$$\Delta T = H(x_b) - Tbb_{obs} \tag{3}$$

where H is RTTOV, x_b is the background field (such as temperature, specific humidity, surface type, surface temperature, surface pressure, 2 m temperature, 2 m specific humidity, 2 m wind, cloud water content, cloud ice water content, cloud cover, cloud top pressure, and total cloud cover; specific details are found in Ding and Wan[12]), and Tbb_{obs} is brightness temperature observed by MODIS. If the initial brightness temperature difference is defined, the observed MODIS brightness temperature is calculated according to Eq. (3). ΔT has a direct impact on the results of assimilation when the background and observation errors are defined in the cost function. In order to increase comparability between the different ideal experiments, the initial ΔT is set to be the same as that shown in Table 3 at each observation point for all the channels. The simulated brightness temperature at each channel is 5 K lower than that observed under clear and partly cloudy conditions, and 5 K higher than that observed under totally cloudy conditions.

Table 3. Initial difference in brightness temperature between background field simulation and observation for ideal tests (unit: K)

Clear sky (Point A)	Total cloud cover (Point B)	Partial cloud cover (Point C)
-5	-5	5

4.1 *Clear sky conditions*

Point A (18° N, 113° E) is located in the sea area and is under clear sky conditions, where cloud water content, cloud ice content, and cloud cover are zero. The radiative transfer model only takes into account the upward atmospheric radiation in the clear sky according to the following equation:

$$L^{Clr}(\nu,\theta) = \tau_s(\nu,\theta)\varepsilon_s(\nu,\theta)B(\nu,T_s) + \int_{\tau_s}^{1} B(\nu,T)d\tau + (1-\varepsilon_s(\nu,\theta))\tau_s^2(\nu,\theta)\int_{\tau_s}^{1}\frac{B(\nu,T)}{\tau^2}d\tau \tag{4}$$

where τ_s is the surface to space transmittance, ε_s is the surface emissivity, $B(\nu,T)$ is the Planck function for frequency (ν) and temperature (T), and τ is the transmittance. When the other parameters are unchanged, the radiance observed by satellite is related

to the vertical distribution of the Planck function and atmospheric transmittance, which are directly related to the distribution of atmospheric temperature and absorbing gases. The main absorption gases for the 16 infrared channels listed in Table 1 are water vapor, CO_2, and ozone. The features of each channel vary widely, and can be used to observe specific physical variables at different altitudes. The only absorption gas considered in this paper is water vapor, which is provided by the WRF model simulation. Other absorption gases, such as CO_2 and ozone, are provided by the standard profiles of RTTOV. Therefore, the assimilation of MODIS radiance in clear sky only influences atmospheric temperature and humidity profiles. The brightness temperature of the 16 MODIS infrared channels is assimilated, which is 5 K higher than that from background simulation (see Table 3). After assimilation, air temperature increased and specific humidity decreased to some extent (Fig. 4). According to Planck's law, atmospheric emissions are enhanced while air temperature increases, leading to a higher satellite-observed brightness temperature. The decrease in humidity reduces the absorption of moisture that can also raise satellite-observed brightness temperature. This shows that the brightness temperature difference is reduced by the process of increasing temperature and deceasing humidity after radiance assimilation, thereby achieving the purpose of data assimilation. The contributions of each channel to temperature and specific humidity vary; however, the characteristics of their distribution are similar with the MODIS weighting functions, which are designed for temperature and humidity observation (see Seemann et al.[14]). This indicates that assimilation results agree with the features of MODIS sensors.

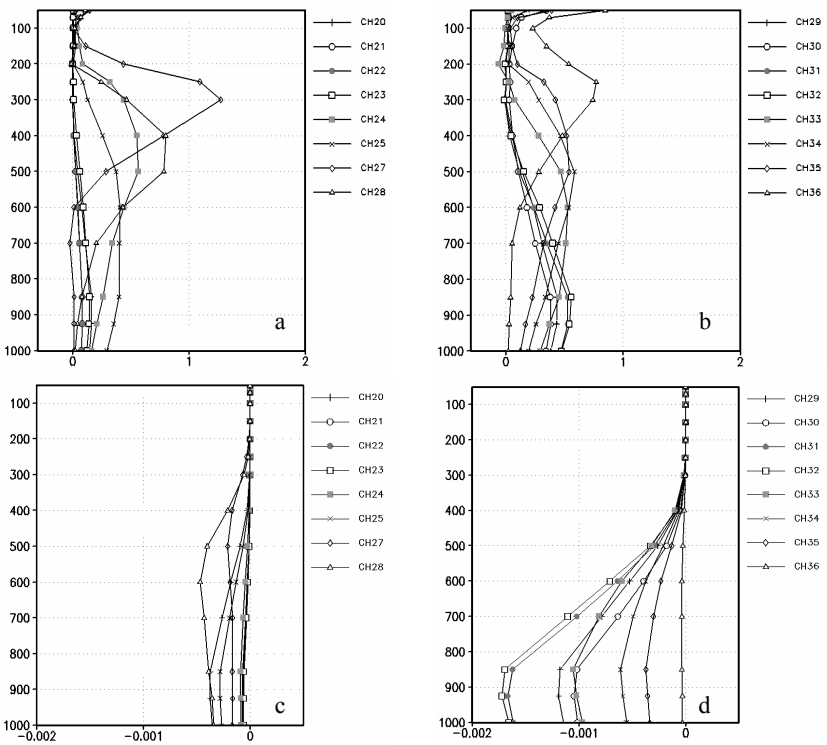

Fig. 4. Changes in temperature (a, b), and specific humidity (c, d) after MODIS radiance assimilation under clear sky conditions

The difference between simulated and observed brightness temperature is reduced for all 16 channels (see Table 4). Maximum reduction is produced after assimilating the radiance of Channels 27 and 28. A comparison of the changes in temperature and specific humidity profiles shows that Channel 27 has the greatest influence on temperature changes, which are mainly located near 300 hPa. Moreover, Channel 28 has a significant impact on 400–500 hPa temperatures. The two channels have more influence on 400–500 hPa specific humidity than other channels. Increasing and decreasing high-level temperature and humidity lead to significant increases in brightness temperature. The main absorption gas of Channels 27 and 28 is water vapor. The purpose of designing these channels is to observe water vapor content in cirrus clouds; hence, they will have significant impact on high-level temperature and humidity after assimilation, which agree with their properties. Channel 29 is also used for water vapor observation; however, according to its weighting function, its observation level is lower than Channels 27 and 28. As such, the levels of its

adjustment are also relatively low, agreeing with its design features. Channels 31 and 32 are window channels, and they can be used to observe surface elements. Thus, they have significant impact on low-level atmospheric temperature and specific humidity after assimilation, which agree with their characteristics.

Table 4. Difference in brightness temperature between field simulation and observation under clear sky conditions (unit: K)

Channel	20	21	22	23	24	25	27	28
ΔT	-4.93	-4.94	-4.94	-4.93	-4.72	-4.76	-2.92	-3.19
Channel	29	30	31	32	33	34	35	36
ΔT	-4.31	-4.47	-3.73	-3.37	-4.06	-4.46	-4.58	-4.43

Difference in brightness temperature slightly decreased after assimilating Channels 20 to 23, and the temperature and specific humidity profiles showed little change (see Fig. 4). Due to the spectrum located on the overlap area of the Sun and the earth-atmosphere radiation system, the radiance received by these channels at daytime consists of the scattering of solar radiation and emission from the earth-atmosphere system, where solar radiation scattering accounts for the most part. Changes in atmospheric temperature and small particles in water vapor have little effect on the scattering of solar radiation under clear sky conditions; hence, impact on temperature and humidity in assimilation is slight.

Water vapor is not the only absorption gas of other channels. For example, the absorption gas of Channels 24, 25, and 33–36 is CO_2, and the absorption gas of Channel 30 is ozone. Although changes in temperature and specific humidity profiles are confirmed with the distribution of weighting function (see Seemann et al.[14]), they need to be further studied. In this paper, CO_2 and ozone use standard profiles in RTTOV, which affect temperature and humidity adjustment.

4.2 *Total cloud cover conditions*

Point B (23° N, 113° E) is located on land, where clouds are mainly located in 500–100 hPa. The maximum cloud cover is equal to 1, and there are cloud ice at high-level.

Assuming black and opaque clouds at a single level, the simulation of cloud-affected radiances is defined as

$$L^{Cld}(\nu,\theta)=\tau_{Cld}(\nu,\theta)B(\nu,T_{Cld})+\int_{\tau_{Cld}}^{1}B(\nu,T)d\tau \quad (5)$$

where $\tau_{Cld}(\nu,\theta)$ is the cloud top to space transmittance and T_{Cld} is the cloud top temperature. The dielectric properties of water and ice are calculated following Liebe[18] and Smith and Shi[19], respectively. They have a consistent random overlap scheme (Raisanen[20]) for clouds. When the observation points are completely covered by clouds, radiations received by the satellites mainly come from the gray clouds above the cloud top; hence, the system can only adjust cloud parameters and parameters in this part of the atmosphere directly after assimilation. However, variables in the 3D variational assimilation system are not independent in the vertical direction, but are influenced by background error covariance matrix. This ensures the consistency of physical variables in the vertical direction. Therefore, according to GRAPES 3D-Var system design, when atmospheric and cloud parameters are adjusted above the cloud top, their impact will spread downwards because of background error covariance.

After each channel assimilation, temperature increases, while specific humidity, cloud cover, and cloud ice water content decrease (Fig. 5). According to the foregoing analysis, the increase in temperature and the decrease in specific humidity increase the simulated brightness temperatures. Meanwhile, the decrease in cloud cover and cloud ice water content lowers cloud top height, leading the satellite to receive more low-level cloud radiation. Moreover, it increases simulated brightness temperatures. This change of atmospheric and cloud parameters eventually increases the simulated brightness temperature, reducing the difference between the observed and simulated brightness temperature.

Channels 27, 28, 35, and 36 have significant impact on temperature, cloud cover, and cloud ice water content near the cloud top. Meanwhile, Channels 27 and 28 adjust cloud specific humidity, which is related to their design properties (see Fig. 5). The point is completely covered by clouds. As such, temperature, cloud ice water content and cloud cover adjustments are mainly located near the cloud top. As they descend from the cloud top, these adjustments will quickly be weakened. However, specific humidity incrementally increases with height reduction. This can be explained by background error covariance. The background field in this experiment does not include cloud water content. Cloud water content in the analyzed field is unchanged after assimilation.

Table 5 shows that ΔT is reduced after assimilation, and the degrees of reduction are higher

than under clear sky conditions. This is mainly due to the adjustment of temperature, cloud ice water content, and cloud cover near the cloud top.

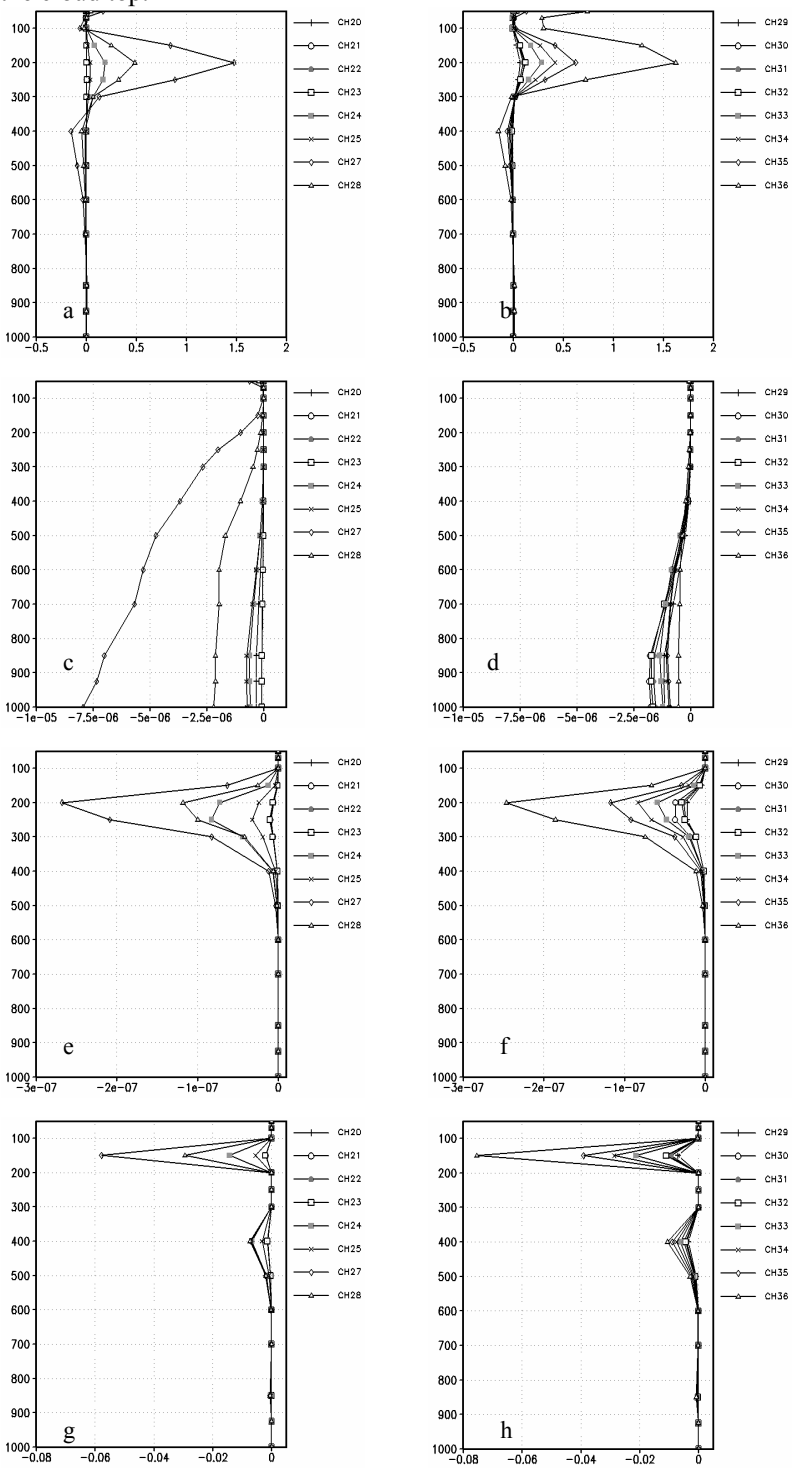

Fig. 5. Changes in temperature (a, b), specific humidity (c, d), cloud ice water content (e, f), and cloud cover (g, h) after the MODIS radiance assimilation under total cloud cover conditions

Table 5. Difference in brightness temperature between field simulation and observation under total cloud cover conditions (unit: K)

Channel	20	21	22	23	24	25	27	28
ΔT	-2.52	-2.44	-2.44	-2.44	-3.3	-1.39	-2.76	-2.3
Channel	29	30	31	32	33	34	35	36
ΔT	-1.56	-1.74	-1.32	-1.28	-1.56	-1.81	-2.17	-3.33

4.3 *Partial cloud cover conditions*

Point C (28°N, 113°E) is located on land, where clouds are mainly located at 300–100 hPa and 925–700 hPa. The maximum cloud cover is less than 1. Cloud ice water content exists at high levels and cloud water content exists at low levels. RTTOV considers clouds as gray bodies (Morcrette)[21]. With the assumption of multi-gray clouds, RTTOV converts radiation calculation for semi-transparent clouds to linear accumulation of clear sky and black-body radiation. In the first two experiments, background simulated brightness temperatures are lower than the observations. However, in this experiment, background simulated brightness temperatures will be 5 K higher than the observations in order to examine the assimilation scheme under partial cloud cover conditions.

Results show that temperature is decreased, while specific humidity, cloud water content, cloud ice water content, and cloud cover are increased (Fig. 6). Such adjustments decrease the simulated brightness temperature, thereby reducing the differences with observed brightness temperature. Characteristics of the vertical adjustment of temperature are similar to that under clear sky conditions, except for the contrary sign. Channel 27 has the maximum adjustment near the cloud top. The specific humidity adjustment is also similar to that under clear sky conditions, but the order of magnitude is smaller. Channels 27 and 28 have significant impact on 500 hPa specific humidity. These characteristics of temperature and specific humidity adjustment show that, under partial cloud cover conditions, low-level atmospheric radiation is transmitted upwards through cloud gaps. Low-level atmospheric parameters can be adjusted after MODIS radiance assimilation under partial cloud cover conditions, which are similar to clear sky conditions. Temperature and specific humidity adjustments at low level are small, compared with adjustments under clear sky. This indicates that cloud cover weakens the effects of satellite data assimilation (Table 6).

To certain degrees, cloud water content, cloud ice content, and cloud cover increase because Channels 23 and 24 have significant impact on cloud water content. There are some distinguishing features of cloud parameters adjustment. For instance, the locations are near clouds, and all channels have similar impact on cloud ice water content, which is greater than cloud water content. High-level and low-level clouds increase at different degrees; Channels 20, 21, 22, and 23 have greater impact on low-level clouds. Adjustments in cloud parameters are consistent with their design properties.

By comparing the simulated brightness temperature with observations, it is found that the simulations are improved in all channels. Channels 27 and 36 have the biggest improvements.

5 CONCLUSIONS AND DISCUSSION

Satellite infrared radiance observations are sensitive to cloud parameters. If the impact of clouds is not taken into account, the radiative transfer model cannot simulate brightness temperature successfully. This leads to the ineffective assimilation of infrared radiance into the initial field of numerical models. In this paper, based on the GRAPES-3D-var system and the characteristics of RTTOV, cloud liquid water, cloud ice water, and cloud cover are added as assimilation variables. Under clear sky, partial cloud cover, and total cloud cover conditions, the brightness temperatures of 16 MODIS channels are respectively assimilated through ideal tests. The results of the ideal tests are as follows:

(1) When the background simulated brightness temperature is lower than the observed temperature, the analyzed field raises the temperature and reduces the moisture, cloud liquid water, cloud ice water, and cloud cover to increase the simulated brightness temperature. A contrary direction adjustment reduces the simulated brightness temperature.

(2) Adjustments in the temperature and moisture under clear sky conditions coincide well with the design of MODIS channels.

(3) Under cloud cover conditions, temperature adjustment is mainly located above the clouds. The impact can spread to lower levels under partial cloud cover conditions. Adjustments in specific humidity are mainly located at the middle and low levels. The impact is largest under clear sky conditions, which declines with the increasing presence of clouds. Cloud parameter adjustments are closely related to background cloud structures; an increase in high-level cloud cover reduces cloud parameter adjustments at lower levels.

(4) Under cloud cover conditions, the 16 MODIS channels have similar impact; Channels 27 and 36 have the greatest impact.

Under total cloud cover conditions, adjustments in physical variables under the clouds depend on the vertical distribution of background error covariance as well as the cross spectrum. A reasonable background error definition can lead to coherence in the assimilation results in vertical direction. Results of this paper agree with the features of the MODIS sensor and the law of meteorology. However, a better scheme may exist, which must be found in the future.

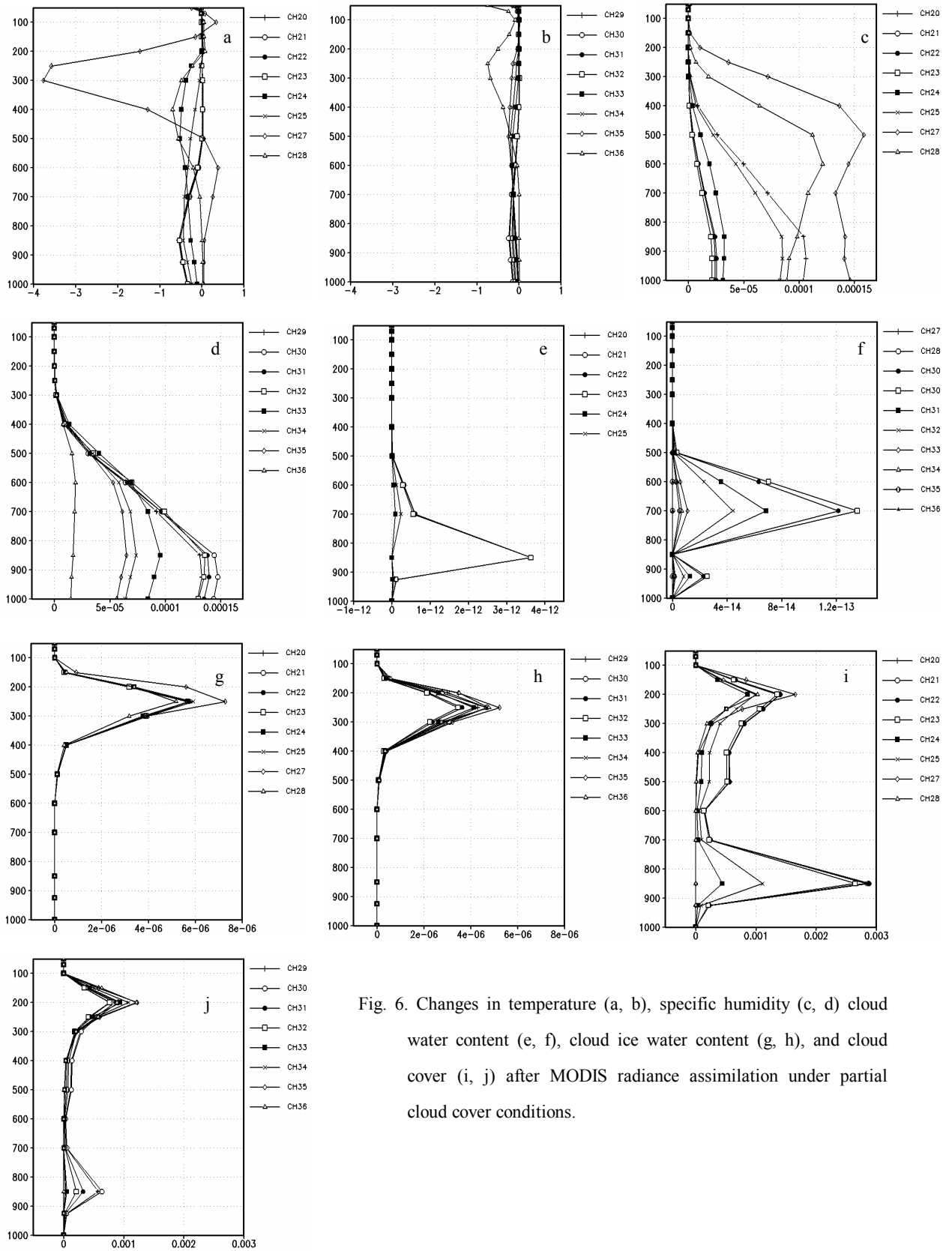

Fig. 6. Changes in temperature (a, b), specific humidity (c, d) cloud water content (e, f), cloud ice water content (g, h), and cloud cover (i, j) after MODIS radiance assimilation under partial cloud cover conditions.

Table 6. Difference in simulated and observed brightness temperature under partial cloud cover conditions (unit: K)

Channel	20	21	22	23	24	25	27	28	29	30	31	32	33	34	35	36
ΔT	4.93	4.93	4.93	4.93	4.76	4.9	2.87	4.24	4.88	4.81	4.82	4.77	4.51	4.33	4.06	2.8

REFERENCES:

[1] DING Wei-yu, WAN Qi-lin, DUAN Yi-hong. 3D-var assimilation of TRMM rain rate and its impact on the typhoon Dujuan (0313) forecast [J]. Chin. J. Atmos. Sci., 2005, 29(4): 600-608.
[2] ZHUANG Zhao-rong, XUE Ji-shan. Assimilation of cloud-derived winds and its impact on typhoon forecast [J]. J. Trop. Meteor., 2004, 20(3): 225-236.
[3] ENTING I G. Inverse problems in atmospheric constituent transport [M]. Cambridge: Cambridge University Press, 2002.
[4] VUKICEVIC T, BRASWELL B H, SCHEIMEL D. A diagnostic study of temperature controls on global terrestrial carbon exchange [J]. Tellus (Serial B), 2001, 53: 150-170.
[5] LI Jun, MENZELB W P, SCHREINERC A J. Variational retrieval of cloud parameters from GOES sounder longwave cloudy radiance measurements [J]. J. Appl. Meteor., 2001, 40(3): 312-330.
[6] ANDERSSON E, PAILLEUX J, THÉPAUT J N, et al. Use of cloud-cleared radiances in three/four-dimensional variational data assimilation [J]. Quart. J. Roy. Meteor. Soc., 1994. 120: 627-653.
[7] OKAMOTO K, DERBER J C. Assimilation of SSM/I radiances in the NCEP global data assimilation system [J]. Mon. Wea. Rev., 2006, 134: 2 612-2 631.
[8] WANG Zong-hao. Direct use of satellite sounding radiances in numerical weather prediction [J]. J. Appl. Meteor. Sci., 1995, 6(1): 101-108.
[9] PAN Ning, DONG Chao-hua, ZHANG Wen-jian. The experiments on direct assimilating atovs radiance [J]. Acta Meteor. Sinica, 2003, 61(2): 226-236.
[10] ZHANG Hua, XUE Jishan, ZHU Guo-fu, et al. Application of direct assimilation of ATOVS microwave radiances to typhoon track prediction [J]. Adv. Atmos. Sci., 2004, 21(2): 283-290.
[11] THOMAS J G, HERTENSTEIN R, VUKIEVI T. An all-weather observational operator for radiance data assimilation with mesoscale forecast models [J]. Mon. Wea. Rev., 2002. 130(7): 1 882-1 897.
[12] DING Wei-yu, WAN Qi-lin. The simulation of CHANCHU typhoon infrared channels [J]. Chin. J. Atmos. Sci., 2008, 32(3): 572-580.
[13] VUKICEVIC T, GREENWALD T, ZUPANSKI M, et al. Mesoscale cloud state estimation from visible and infrared satellite radiances [J]. Mon. Wea. Rev., 2004, 132(12): 3 066-3 077.
[14] SEEMANN S W, LI J, MENZEL W P, et al. Operational retrieval of atmospheric temperature, moisture, and ozone from MODIS infrared radiances [J]. J. Appl. Meteor., 2003, 42: 1 072-1 091.
[15] BORMANN N, THÉPAUT J-N. Impact of MODIS polar winds in ECMWF's 4DVAR data assimilation system [J]. Mon. Wea. Rev., 2004. 132(4): 929-940.
[16] JAKOB C. Cloud cover in the ECMWF reanalysis [J]. J. Climate, 1999, 12(4): 947-959.
[17] PARK S K, DROEGEMEIER K. Sensitivity analysis of a 3D convective storm: implications for variational data assimilation and forecast error [J]. Mon. Wea. Rev., 2000, 128(1): 140-159.
[18] LIEBE H J. MPM-an atmospheric millimeter-wave propagation model [J]. Int. J. Infrared Millim. Waves, 1989, 10(6): 631-650.
[19] SMITH E A, SHI L. Surface forcing of the infrared cooling profile over the Tibetan plateau Part I: Influence of relative longwave radiative heating at high altitude [J]. J. Atmos. Sci., 49: 805-822.
[20] RAISANEN P. Effective longwave cloud fraction and maximum-random overlap of clouds: A problem and a solution[J]. Mon. Wea. Rev., 1998, 126, 3 336-3 340.
[21] MORCRETTE J J. Radiation and cloud radiative properties in the ECMWF forecasting system [J]. J.Geophys. Res., 1991, 96(D): 9 121-9 132.

Citation: DING Wei-yu, WAN Qi-lin, ZHANG Chen-zhong et al. MODIS brightness temperature data assimilation under cloudy conditions: Methods and ideal tests. *J. Trop. Meteor.*, 2010, 16(4): 313-324.